Pulmonary Circulation

WILEY

PVRi | Pulmonary Circulation Open Access

RESEARCH ARTICLE OPEN ACCESS

Role of MiR-542-3p/Integrin-Linked Kinase/Myocardin Signaling Axis in Hypoxic Pulmonary Hypertension

Linqing Li[1] | Weining Zhou[2] | Qingrong Ji[1] | Xianzhao Zhang[1] | Ni Yang[1] | Kaiyou Song[1] | Shunpeng Hu[1] | Cunfei Liu[1] | Zhihong Ou[1] | Fengwei Zhang[3] | Yuda Wei[4] | Jiantong Hou[1]

[1]Department of Cardiology, Linyi People's Hospital, Linyi, China | [2]Department of Pathology, Linyi People's Hospital, Linyi, China | [3]Department of Cardiac Surgery, Linyi People's Hospital, Linyi, China | [4]Key Laboratory for Laboratory Medicine of Linyi City, Department of Laboratory Medicine, Linyi People's Hospital, Linyi, China

Correspondence: Jiantong Hou (bigbang89757@126.com)

Received: 19 November 2024 | **Revised:** 24 April 2025 | **Accepted:** 25 April 2025

Funding: This study was supported by the National Natural Science Foundation of Shandong Province (ZR2021QH312).

Keywords: hypoxic pulmonary hypertension | integrin-linked kinase | MiR-542-3p | phenotypic transition | pulmonary artery smooth muscle cells

ABSTRACT

Phenotypic transition of pulmonary artery smooth muscle cells (PASMCs) under hypoxic conditions, which in turn causes increased proliferation and migration capacity, is an important pathological process in Hypoxic pulmonary hypertension (HPH). Although research on the phenotypic transition of PASMCs has been ongoing, little is known about the specific molecular mechanisms underlying this process. Integrin-linked kinase (ILK) is one of the genes essential for maintaining the contractile phenotype of vascular smooth muscle cells (VSMCs). It has been shown that ILK is a target gene of MiR-542-3p, and overexpression of MiR-542-3p can promote apoptosis of osteosarcoma cells by downregulating the expression of ILK, and inhibit their cell proliferation, migration, and invasion. In this study we found that hypoxia upregulated MiR-542-3p expression, and MiR-542-3p mimics reduced ILK, Myocardin expression, and promote phenotypic transition in PASMCs. And, ILK was a direct target of MiR-542-3p in PASMCs. MiR-542-3p inhibitor reversed hypoxia-induced reduction of ILK and Myocardin expression in PASMCs, and phenotypic transition, proliferation, and migration of PASMCs. MiR-542-3p antagomir reversed hypoxia-induced pulmonary vascular remodeling and also reversed hypoxia-induced reduction in ILK, Myocardin expression, and phenotype transition in rat pulmonary arteries. Thus, our results suggest that hypoxia induced an increase in MiR-542-3p expression, which caused an increase in binding to ILK gene and negatively regulated ILK expression. This in turn, caused a decrease in Myocardin expression leading to phenotypic transition, proliferation, and increased migration of PASMCs, causing hypoxic pulmonary vascular remodeling and ultimately leading to HPH.

1 | Introduction

Hypoxic pulmonary hypertension (HPH) is one of the complications of chronic hypoxic lung disease, which is mainly due to various causes of alveolar hypoxia [1]. The pathogenesis of HPH is complex, and it has not yet been possible to fully elucidate its specific pathogenesis. Hypoxic pulmonary vascular remodeling is an important pathological basis for the development of HPH. Pulmonary artery smooth muscle cells (PASMCs), as a major component of the pulmonary vasculature, are key players in hypoxic pulmonary vascular remodeling. PASMCs undergo a phenotypic transition from a contractile phenotype to a synthetic phenotype under hypoxic conditions, resulting in enhanced proliferation and migration, and this process is the initiator of hypoxic pulmonary vascular remodeling [2].

Although research on the phenotypic transition of PASMCs has been ongoing, little is known about the specific molecular mechanisms underlying this process.

Integrin-linked kinase (ILK) is a serine/threonine protein kinase, a cross-linked structural protein that connects integrins to growth factor signaling pathways. It is widely found in various cell types and plays a vital role in transmitting cell signaling information. ILK mediates intra- and extracellular signaling through binding to integrins to regulate cell growth, survival, proliferation, and migration [3]. We previously found that early hypoxia induces a decrease in ILK kinase activity, which in turn decreases the binding of Myocardin to the promoter of the SM α-actin gene, thereby regulating the phenotypic transition of PASMCs at the gene level. Chronic hypoxia reduces ILK and Myocardin expression, and reduced ILK expression reduces Myocardin levels, thereby contributing to the phenotypic transition of PASMCs at the protein level [4]. This suggests that ILK plays a key role in pulmonary vascular remodeling. However, the pathway through which hypoxia reduces ILK expression remains unknown.

MicroRNAs (MiRNAs) are small endogenous noncoding RNAs of about 22 nucleotides in length, which regulate the expression of target genes by directly binding to the 3′-untranslated region of mRNAs, inhibiting their translation and/or promoting their degradation [5]. Currently, several MiRNAs have been shown to be closely related to the development of HPH [6]. It has been shown that MiR-497, MiR-1268a, and MiR-665 are novel hypoxia-associated MiRNAs, which are involved in regulating the proliferation of PASMCs by directly regulating the expression of p15, p16, and p21 [7]. Therefore, it may be possible to elucidate the mechanism of phenotypic transition and proliferative migration of PASMCs from the perspective of MiRNA. We found that MiR-542-3p could binds to the 3′-UTR region of the ILK coding gene as predicted by TargetScans Biology software. Moreover, previous studies have shown that MiR-542-3p levels are significantly elevated in patients with chronic obstructive pulmonary disease (COPD), and more so in patients with severe COPD [8]. This suggests that MiR-542-3p may be involved in the development of pulmonary vascular remodeling by regulating ILK.

In our study, we explored the role of MiR-542-3p/ILK/Myocardin signaling axis in the HPH. We hypothesized that MiR-542-3p reduces ILK expression by binding to the ILK gene, which in turn reduces Myocardin expression and ultimately causes pulmonary vascular remodeling. To verify this hypothesis, we determined the role of MiR-542-3p in the phenotypic transition and proliferative migration of PASMCs by using MiR-542-3p mimics and inhibitors, among other methods. Our results provide novel therapeutic targets for preventing and treating HPH.

2 | Materials and Methods

2.1 | Cell Culture

Rat PASMCs were isolated from pulmonary arteries of male Sprague–Dawley rats (weight, 150–180 g) as described [4]. In brief, the rats were killed by intraperitoneal injection of pentobarbital sodium (150 mg/kg) and the pulmonary arteries were quickly removed and placed in the medium. The remaining pulmonary artery membranes were cut into $1 \times 1 mm^2$ with ophthalmic scissors and then transferred to the culture flask. The PASMCs were cultured in DMEM/F12 (Hyclone, Logan, UT, USA) medium supplemented with 20% FBS and 1% penicillin and streptomycin (Invitrogen, Carlsbad, CA, USA). PASMCs were cultured for a week, and medium was changed every 3 days. The results of the identification of PASMCs are presented in the Figure S1. All experiments were performed with cells at passages 1–2. PASMCs were subjected to different hypoxic time interventions (12, 24, 48 h). The experiment was conducted after PAMSCs were starved for 24 h in 0.1% FBS medium. The cells were placed in a hypoxia incubator containing 1% O_2 and 5% CO_2 at 37°C for the hypoxia experiments.

2.2 | Transfection of miRNA Mimics and Inhibitor and Hypoxia Treatment

PASMCs were seeded in 12-well plates and were transfected with 100 nM MiR-542-3p mimics, inhibitor, or negative control (NC) (RiboBio Guangzhou, China) at 50% cell density using Lipofectamine RNAiMAX transfection reagent (Thermo Scientific, USA) and Opti-MEM (Gibco BRL, USA) culture medium according to the manufacturer's protocol. Cells were treated with hypoxia 48 h after transfection. PASMCs were subjected to different hypoxic time interventions (12, 24, 48 h). The experiment was conducted after PAMSCs were starved for 24 h in 0.1% FBS medium. The cells were placed in a hypoxia incubator containing 1% O_2 and 5% CO_2 at 37°C for the hypoxia experiments.

2.3 | Immunofluorescence

PASMCs were washed with phosphate-buffered saline (PBS) and fixed with 4% paraformaldehyde at room temperature for 20 min. Cells were treated with 0.2% Triton X-100 followed by blocking with 5% BSA. Then cells were incubated with anti-ILK (611803; BD Biosciences, Franklin Lakes, NJ, USA) overnight at 4°C after which samples were incubated with Alexa Fluor 555-conjugated second antibody for 1 h at room temperature. Finally, the cells were stained with DAPI, and observed under microscope (Olympus IX71, Tokyo, Japan).

2.4 | Luciferase Reporter Assay

The wild-type (WT) 3′-UTR or mutated (Mut) 3′-UTR of LK was inserted downstream of the firefly luciferase gene in the psiCHECK-2 (Promega, USA) plasmid. PASMCs were transfected with WT or Mut plasmid using Lipofectamine RNAiMAX transfection reagent (Thermo Scientific, USA), and then the cells were transfected with MiR-542-3p mimics or NC mimics, respectively. Cells were harvested 48 h posttransfection and analyzed using a dual-luciferase reporter gene assay kit (Yeasen Biotech, China) according to the manufacturer's instructions. The firefly luciferase activity was normalized to the Renilla luciferase activity.

2.5 | Western Blot Analysis

Total proteins were extracted with RIPA buffer (ShineGene; Molecular Biotech Inc., Shanghai, China). Total protein concentration was measured using the BCA Protein Assay Kit (Pierce

Chemical Co., Rockford, IL, USA). Equal amounts of total protein (50–100 μg) were subjected to 10% sodium dodecyl sulfate-polyacrylamide gel electrophoresis (SDS-PAGE) and electro-transferred onto PVDF membranes (Millipore, Billerica, MA, USA). The PVDF membranes were blocked in 5% nonfat powdered milk and probed with primary antibodies overnight. The primary antibodies used in this experiment included anti-ILK (ab52480; Abcam), anti-myocardin (SAB4200539; Sigma, St. Louis, MO, USA), anti-SM α-actin (ab7817; Abcam), anti-calponin (ab46794; Abcam), anti-osteopontin (ab8448; Abcam), and anti-β-actin (cst-8457; Cell Signaling Technology, Danvers, MA, USA). The PVDF membranes were incubated with secondary antibody (Beijing TDY Biotech Co. Ltd., Beijing, China) for 2 h at room temperature. The ECL Western blot analysis System (DH0101; Donghuan, Shanghai, China) was used to expose the immunoreactive bands. The bands were analyzed using the ChemiDoc MP imaging system (BioRad Laboratories Inc., Hercules, CA, USA). All experiments were repeated at least three times.

2.6 | Real-Time Quantitative PCR Assay

TRIzol reagent (Invitrogen) was used to extract total RNA from PASMCs or according to the manufacturer's instructions. The NanoDrop ND-1000 spectrophotometer (Thermo Fisher Scientific, Waltham, MA, USA) was used to measure total RNA concentration. cDNA was synthesized by using SuperScript III reverse transcriptase (Invitrogen). Real-time PCR was conducted using the Prism 7500 SDS (Applied Biosystems/Thermo Fisher Scientific Inc.) and SYBR Green I (SYBR Green I Supermix; Bio-Rad Laboratories). The PCR primers for MiR-542-3p were forward primer: 5′-GTCGTATCCAGTGCAGGGTCCGAGGTATTCGCACTGGATACGACTTTCAGTT-3′, and reverse primer: 5′-TGTGACAGATTGATAACTGAAA-3′.'The PCR primers for ILK were forward primer: 5′-TGGACGACATTTTCACTCA-3′, and reverse primer: 5′-CTGATTTAGGTCGTTCTCTGTGT-3′. The PCR primers for myocardin were forward primer: 5′-TCGCCTAACAACCATTACTTC-3′, and reverse primer: 5′-CTGGCATTTCTCCACTTTCA-3′. The PCR primers for SM α-actin were forward primer: 5′-AACTGGTATTGTGCTGGACTCTG-3′, and reverse primer: 5′-CTCAGCAGTAGTCACGAAGGAATA-3′. The PCR primers for calponin were forward primer: 5′-AGGTCAATGAGTCAACCCAGAAC-3′, and reverse primer: 5′-CCTGCTGACTGGCAAACTTATT-3′. The PCR primers for osteopontin were forward primer: 5′-GATGAACAGTATCCCGATGCCA-3′, and reverse primer: 5′-GTCTTCCCGTTGCTGTCCTGA-3′. The PCR primers for GAPDH were forward primer: 5′-CTGGAGAAACCTGCCAAGTATG-3′, and reverse primer: 5′-GGTGGAAGAATGGGAGTTGCT-3′. The PCR primers for U6 were forward primer: 5′- CTCGCTTCGGCAGCACA-3′, and reverse primer: 5′-AACGCTTCACGAATTTGCGT-3′. An endogenous reference gene (GAPDH or U6) was used as a control for expression of the target gene, and the relative expression of mRNA of the target gene was determined by the $2^{-\Delta\Delta Ct}$ calculation.

2.7 | Wound Healing Assay

PASMCs were seeded in 6-well plates at 1.0×10^6 cells per well. After cells were grown to confluence, the cell monolayer was scraped with a pipette tip to create a scratch, washed three times with PBS and cultured in FBS-free medium. Cells were imaged, and the scratch area was measured using ImageJ image analysis software (version 1.51J8, Bethesda, USA).

2.8 | 3-(4,5-Dimethyl-2-Thiazolyl)-2,5-Diphenyl-2-H-Tetrazolium Bromide (MTT) and Enzyme-Linked Immunosorbent Assay (ELISA)

The extracted rat blood was centrifuged at 3000 rpm/min for 20 min using a high-speed centrifuge, and the supernatant was collected for ELISA determination of ILK concentration. Sample dilutions were added to the sample wells to be tested, followed by the samples to be tested. The enzyme plate was placed in a thermostatic incubator at 37°C for 30 min, followed by washing and addition of enzyme reagents. Each well was added with colorant to develop the color at 37°C for 15 min under light protection, followed by the addition of termination solution to terminate the reaction. Finally, the optical density (OD) of each well was measured at 450 nm. For MTT assay, 10 μL of MTT solution was added to the 96-well plate, followed by incubation in a CO_2 incubator for 4 h. 100 μL of Formazan solubilization solution was added to each well, followed by further incubation in a CO_2 incubator for 3–4 h until all the purple crystals were observed to be dissolved under a light microscope. The absorbance at 570 nm was subsequently measured using an enzyme meter.

2.9 | Animal Grouping and HPH Model Construction

Male Sprague–Dawley rats (weight, 150–180 g) were obtained from the Linyi People's Hospital Animal Center. Twenty-four rats were divided into four groups of six rats: (1) Control, (2) negative control (NC) antagomir, (3) NC antagomir + hypoxia, and (4) MiR-542-3p antagomir + hypoxia. The rat HPH model was established as previously described [4]. MiR-542-3p antagomir (10 mg/kg) or MiR-542-3p NC was injected through the tail vein, and then the rats in the hypoxia group were placed in a fully automated hypoxia chamber, maintaining an O_2 concentration of 10% in the chamber, and were subjected to intermittent hypoxia for 8 h per day for 4 weeks. Meanwhile, rats were exposed to normoxia (21% O_2) in the control group. The animals were housed in a vivarium under controlled photocycle (12 h light/12 h dark) and temperature (22°C–25°C) conditions with free access to food and water.

2.10 | Determination of Hemodynamics and Right Ventricular Hypertrophy Index

The method for determining the mean pulmonary artery pressure (mPAP) in rats as previously described [4]; the mPAP was monitored using an intra-arterial fluid-filled catheter connected to RM6240BD physiological multichannel recorder. The rats were killed by intraperitoneal injection of pentobarbital sodium (150 mg/kg) after determination of mPAP. The heart and lungs of the rats were removed from the chest and then washed with

physiological saline. Rat right ventricle (RV), left ventricle (LV), and septum (S) were separated and weighed to calculate RV/(LV + S) to assess right ventricular hypertrophy. Rat pulmonary arteries were subjected to western blot analysis and Real-time PCR analysis. Rat serum was subjected to ELISA and Real-time PCR analysis.

2.11 | Hematoxylin and Eosin (H and E) Staining

Lungs were removed from rats and placed in 4% paraformaldehyde for 24 h, followed by paraffin embedding and sectioning. Lung specimens were then stained with H and E. Six nonoverlapping visual fields were randomly selected for microphotographs under 400× magnification. The pulmonary arterioles with a diameter of 100–200 μm were analyzed by using Image-ProPlus 6.0. The percentage of medial wall thickness (WT%) and wall area (WA%) of pulmonary arteries was calculated to assess pulmonary vascular remodeling.

2.12 | Statistical Analyses

Data are expressed as mean ± standard deviation and analyzed using SPSS17.0 software (SPSS Inc., Chicago IL, USA). The independent samples *t*-test was used for comparison between the two groups, and one-way analysis of variance was used to compare the groups. *p*-values < 0.05 were considered statistically significant.

3 | Results

3.1 | Hypoxia Promotes MiR-542-3p Expression in PASMCS

To investigate the effects of hypoxia on MiR-542-3p expression in PASMCs, we designed different hypoxia time gradients (0, 12, 24, 48 h). We found that the expression of MiR-542-3p were increased in a time-dependent manner after hypoxia for 12, 24, and 48 h ($p < 0.05$) (Figure 1A).

3.2 | MiR-542-3p Mimics Reduces ILK, Myocardin Expression and Promote Phenotypic Transition in PASMCs

Our previous study has demonstrated that hypoxia for 24 h downregulated the expression of ILK, myocardin, and the PASMC contraction phenotype marker proteins SM α-actin and calponin, while increasing the expression of the PASMC synthesis phenotype marker protein osteopontin [4]. This process is termed hypoxia-induced phenotype transition in PASMCs. To investigate the effect of MiR-542-3p on ILK, Myocardin expression and phenotypic transition in PASMCs, we performed Western blot and immunofluorescence analyses. We found that ILK and Myocardin expression were significantly reduced in PASMCs transfected with MiR-542-3p mimics. In addition, MiR-542-3p mimics significantly promoted phenotypic transition in PASMCs ($p < 0.05$)

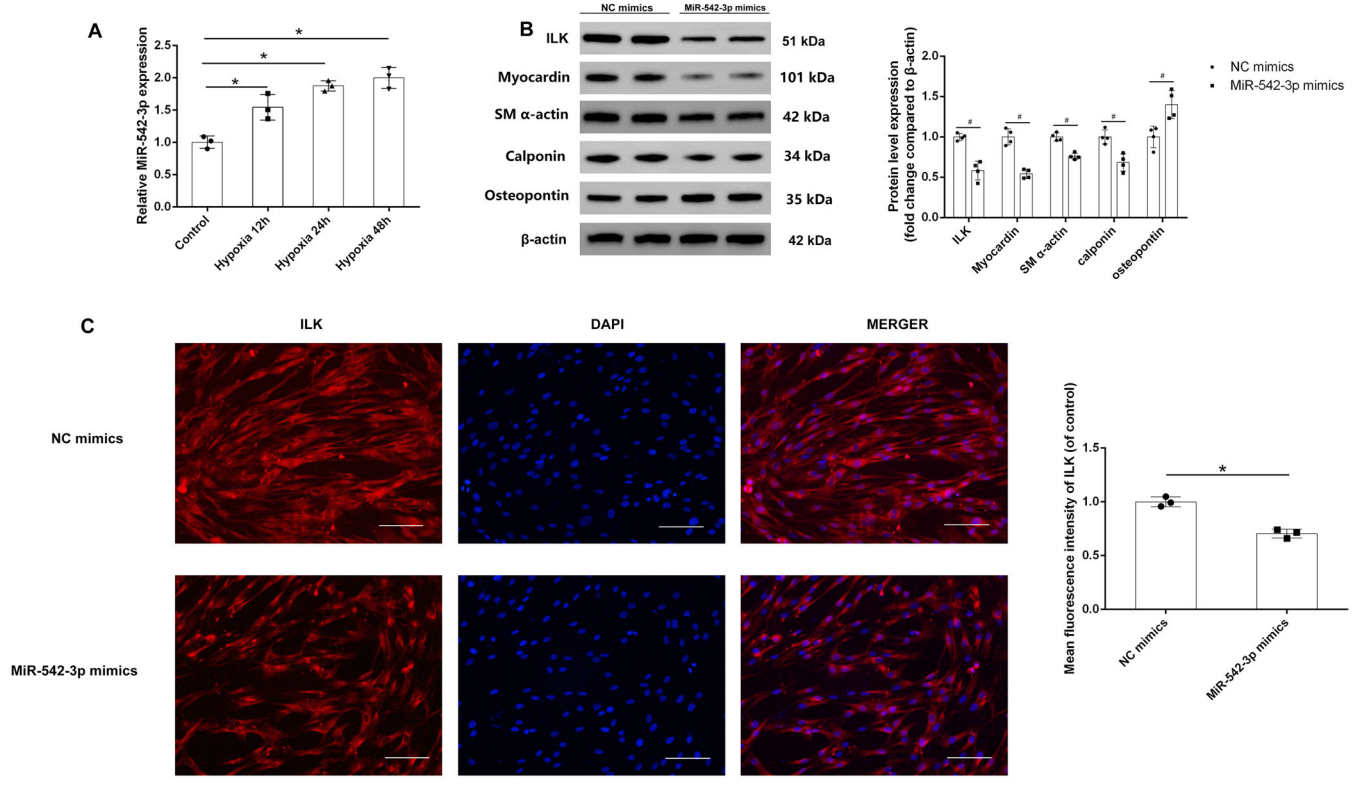

FIGURE 1 | Effects of different hypoxia times on MiR-542-3p expression and MiR-542-3p on ILK, Myocardin expression and promotion of phenotypic transition in PASMCs. Relative expression of MiR-542-3p using Real-time quantitative PCR (A). Representative Western blots and quantification of ILK, Myocardin, and marker gene by densitometry (B). Immunofluorescence of ILK expression in PASMCs (C). Data are expressed as means ± standard deviation. ($n \geq 3$; $^{*}p < 0.05$ compared with Control and NC mimics; $^{\#}p < 0.05$ compared with NC mimics; scale bar, 100 μm).

(Figure 1B). The results of immunofluorescence were consistent with Western blot analyses ($p < 0.05$) (Figure 1C).

3.3 | ILK Was a Direct Target of MiR-542-3p in PASMCs

To verify whether ILK is a target gene of MiR-542-3p in PASMCs, we performed dual-luciferase reporter assay. PASMCs were cotransfected with the WT or Mut reporter plasmids and the MiR-542-3p mimics or negative control (NC) mimics (Figure 2A). After transfection for 48 h, luciferase activity was measured by a dual-luciferase reporter assay kit. We found that transfection of MiR-542-3p mimics significantly reduced luciferase activity in PAMSCs ($p < 0.05$) (Figure 2B).

3.4 | MiR-542-3p Inhibitor Reverses Hypoxia-Induced Reduction of ILK, Myocardin Expression and Phenotype Transition in PASMCs

PASMCs were transfected with the MiR-542-3p inhibitor construct to determine if inhibiting MiR-542-3p prevents downregulation of ILK, myocardin, and the phenotype transition after 24 h of hypoxia in PASMCs. We found that MiR-542-3p inhibitor significantly reversed the hypoxia 24 h-induced reduction in ILK and Myocardin expression and phenotype transition in PASMCs. ($p < 0.05$) (Figure 3A,B). The results of real-time PCR were consistent with Western blot analyses ($p < 0.05$) (Figure 3C).

3.5 | MiR-542-3p Inhibitor Reverses Hypoxia-Induced Migration and Proliferation of PASMCs

Increased migration and proliferation of PASMCs are a fundamental pathological process in pulmonary vascular remodeling. To investigate the effect of MiR-542-3p on the proliferation and migration of PASMCs, we performed wound healing and MTT assay. We found that hypoxia for 24 h significantly promoted migration and proliferation of PASMCs, however, transfection with MiR-542-3p inhibitor significantly reversed this trend ($p < 0.05$) (Figure 4A–C).

3.6 | MiR-542-3p Antagomir Reverses Hypoxia-Induced Pulmonary Vascular Remodeling

To investigate the effects of MiR-542-3p on pulmonary vascular remodeling, we established a rat model of pulmonary hypertension by hypoxia for 4 weeks. We found that mPAP and RV/(LV + S) were significantly increased in the NC antagomir + Hypoxia group compared with the NC antagomir group. However, the use of MiR-542-3p antagomir significantly reversed hypoxia-induced increased levels of mPAP and RV/(LV + S) in rats ($p < 0.05$) (Figure 5A,B). To evaluate the effect of hypoxia on pulmonary vascular remodeling, we performed hematoxylin and eosin staining of pulmonary arteries (Figure 6A). The WT% and WA% in the NC antagomir + Hypoxia group were significantly increased compared with the NC antagomir group. However, hypoxia-induced increases in WT% and WA % are significantly reversed in MiR-542-3p antagomir + Hypoxia group ($p < 0.05$) (Figure 6B).

3.7 | MiR-542-3p Antagomir Reverses Hypoxia-Induced Reduction of ILK and Myocardin Expression in Pulmonary Arteries

We performed Western blot analysis and RT-PCR to investigate the effects of MiR-542-3p on ILK and Myocardin in pulmonary arteries. We found that ILK and myocardin expression decreased in NC antagomir + Hypoxia compared with the NC antagomir group. However, the use of MiR-542-3p antagomir significantly reversed hypoxia-induced increased levels of ILK and Myocardin expression in pulmonary arteries ($p < 0.05$) (Figure 7A–C).

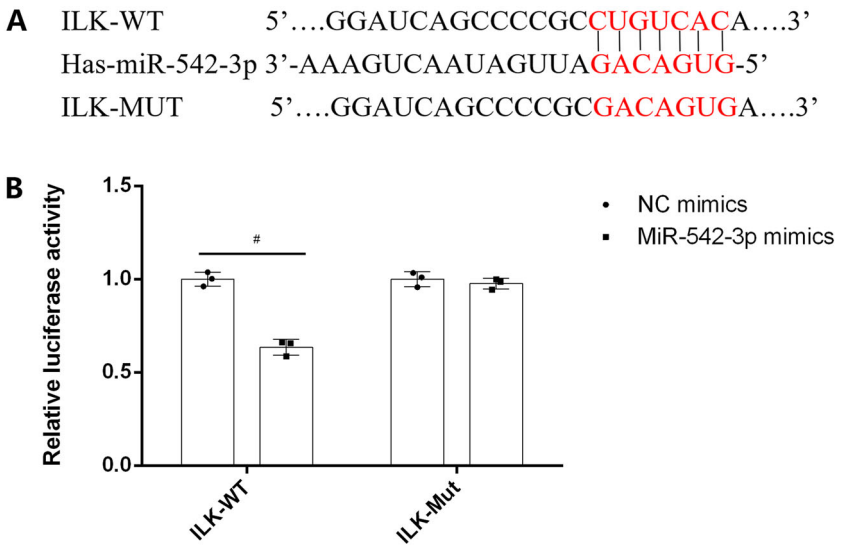

FIGURE 2 | ILK was a direct target of MiR-542-3p in PASMCs. The 3′-UTR of ILK contained a candidate binding site for MiR-542-3p (A). The wild-type (WT) 3′-UTR or mutated (Mut) 3′-UTR of ILK was inserted downstream of the firefly luciferase gene. PASMCs were cotransfected with the WT or Mut reporter plasmids and the MiR-542-3p mimics or negative control (NC) mimics. After transfection for 48 h, luciferase activity was measured by a dual-luciferase reporter assay kit (B). Data are expressed as means ± standard deviation. $n = 3$; $^{\#}p < 0.05$ compared with NC mimics.

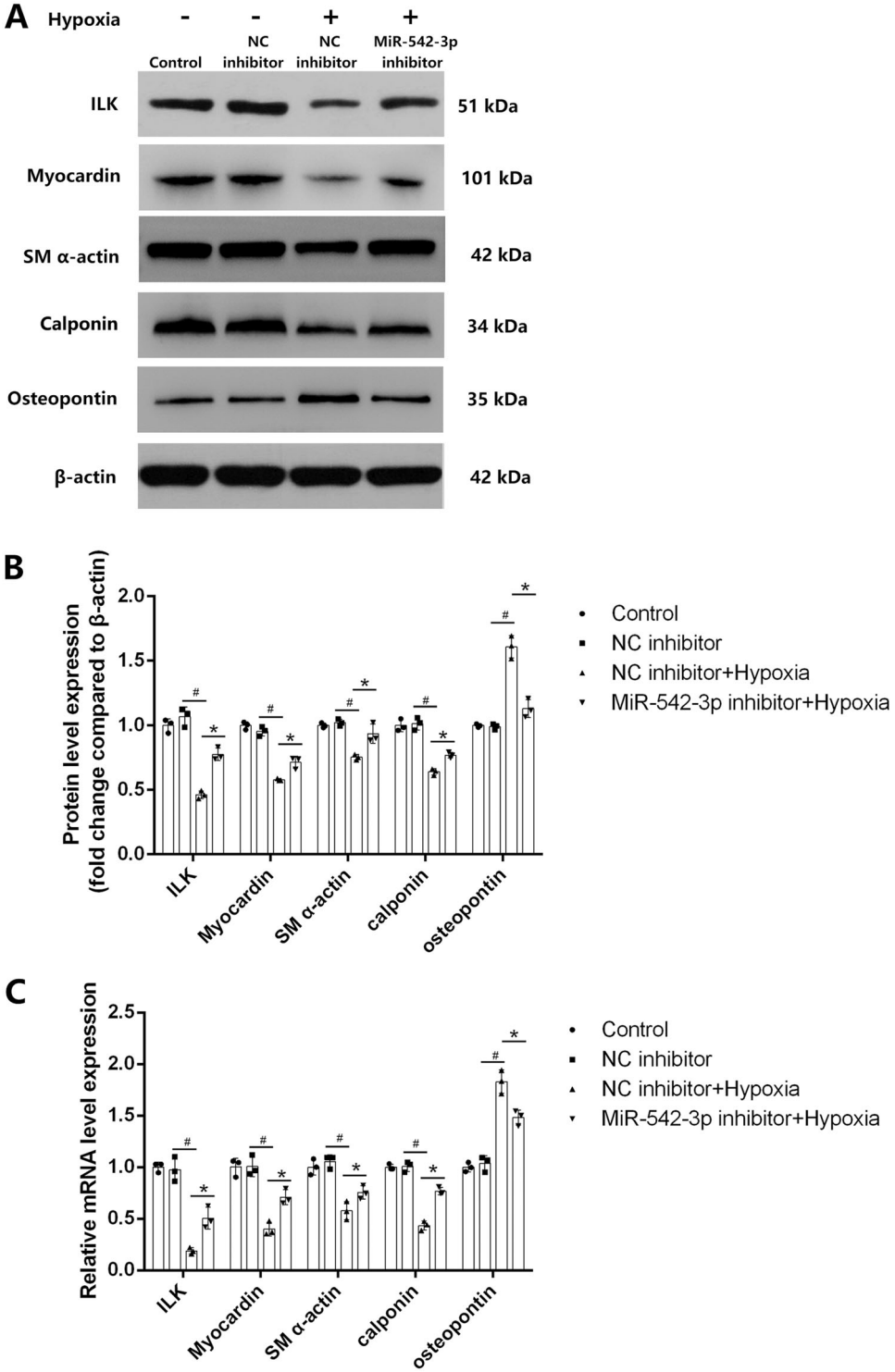

FIGURE 3 | Effects of MiR-542-3p on ILK, Myocardin, and PASMC marker proteins expression under hypoxic conditions in PASMCs. Representative Western blots (A). Quantification of these factors by densitometry (B). Changes in mRNA expression of these factors (C). Data are expressed as means ± standard deviation. $n = 3$; $^{\#}p < 0.05$ compared with NC inhibitor. $^{*}p < 0.05$ compared with NC inhibitor + hypoxia group.

3.8 | MiR-542-3p Antagomir Reverses Hypoxia-Induced Reduction of ILK Concentration in Rat Serum

The use of MiR-542-3p antagomir significantly reversed hypoxia-induced increase of MiR-542-3p expression in rat serum ($p < 0.05$) (Figure 7D). We performed ELISA to investigate the effects of MiR-542-3p on ILK concentration in rat serum. We found that hypoxia induced a decrease in serum ILK concentration in rats. The use of MiR-542-3p antagomir significantly reversed hypoxia-induced reduction of ILK concentration in rat serum ($p < 0.05$) (Figure 7E).

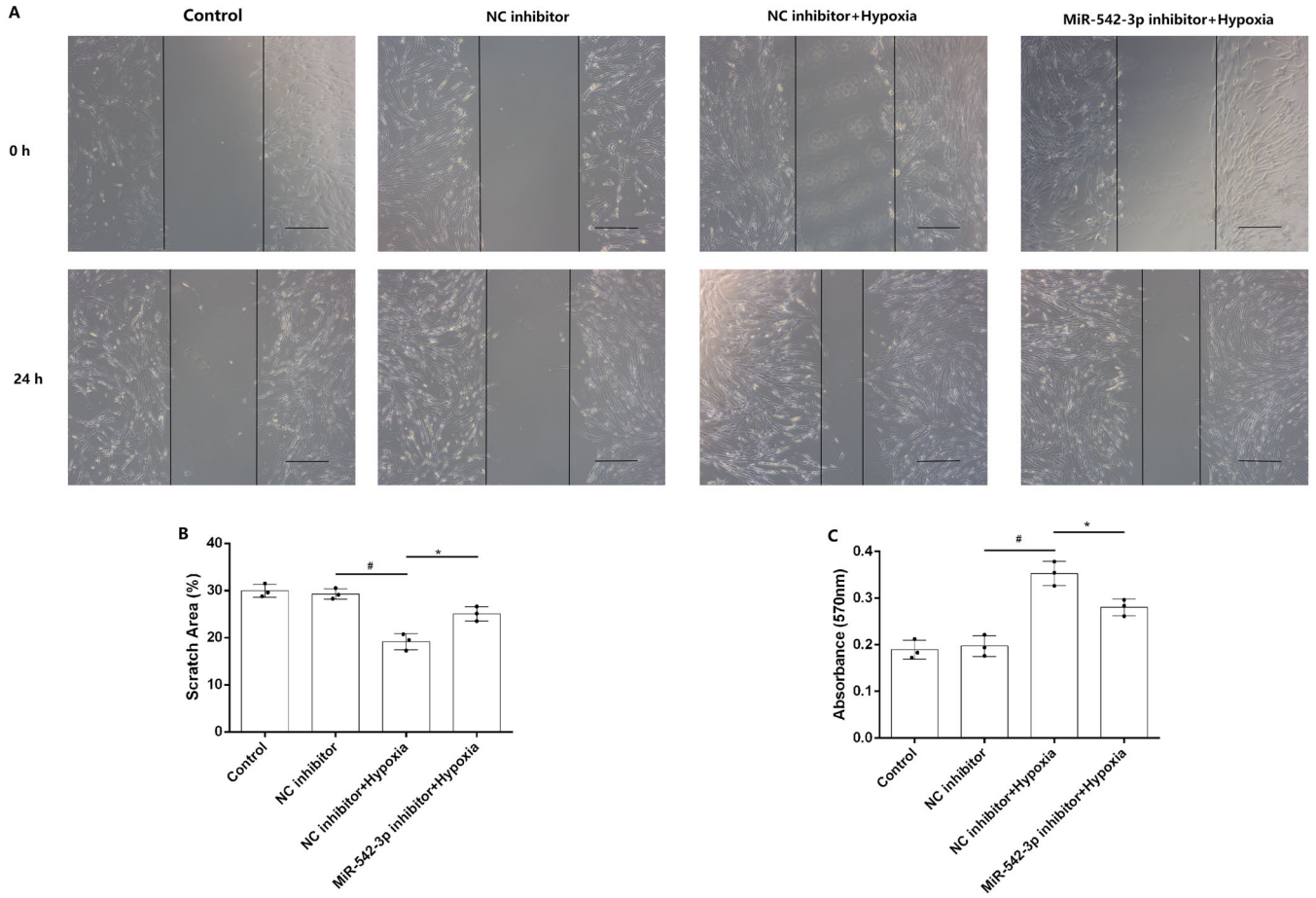

FIGURE 4 | Effects of MiR-542-3p on migration and proliferation of PASMCs. Wound healing assay for cell migration in PASMCs (A). Quantification of scratch area in PASMCs (B). Cell viability was determined using MTT assays of PASMCs (C). Data are expressed as means ± standard deviation. $n = 3$; $^{\#}p < 0.05$ compared with NC inhibitor. $^{*}p < 0.05$ compared with NC inhibitor + hypoxia group. Scale bar, 200 μm.

3.9 | MiR-542-3p Antagomir Reverses Hypoxia-Induced Phenotype Transition in Pulmonary Arteries

We performed Western blot analysis to investigate the effects of MiR-542-3p antagomir on phenotype transition in pulmonary arteries. We found that SM α-actin and calponin expression decreased in NC antagomir + Hypoxia compared with the NC antagomir group. However, osteopontin expression was significantly elevated in NC antagomir + Hypoxia compared with the NC antagomir group. The use of MiR-542-3p antagomir significantly reversed hypoxia-induced phenotype transition in pulmonary arteries ($p < 0.05$) (Figure 7F,G).

4 | Discussion

This is the first research to confirm the effect of MiR-542-3p/Integrin-linked kinase/Myocardin signaling axis in HPH. We found that MiR-542-3p reduces ILK expression by binding to the ILK gene, which in turn reduces Myocardin expression and ultimately causes pulmonary vascular remodeling. This further revealed the specific molecular mechanism of HPH. This indicated that MiR-542-3p might be a potential biomarker for the assessment of risk of HPH, as well as serving as a novel therapeutic target.

HPH is a group of progressive clinical syndromes with high mortality caused by chronic hypoxia. It is characterized by endothelial dysfunction and pulmonary vascular remodeling caused by excessive proliferation of the vascular wall, which leads to increased pulmonary vascular resistance and decreased compliance, resulting in right heart failure [9]. The pathogenesis of HPH is complex and has not been fully elucidated, although much progress has been made in the last decades, and there is no effective radical treatment other than lung transplantation [10, 11]. Lung transplantation cannot be fully carried out due to the high cost of treatment, high surgical risk, and shortage of donors. Therefore, it is extremely important to explore the pathogenesis of HPH to provide an effective means of prevention and treatment.

COPD, interstitial lung disease, and alveolar hypoxia caused by prolonged exposure to high altitude are important etiologic factors in the development of HPH [12]. Hypoxic pulmonary vascular remodeling caused by chronic hypoxia is an important pathological process in the development of HPH. Existing studies have shown [13–16] that endothelial-to-mesenchymal transition (EndMT), phenotypic transition of PASMCs, increased proliferation and migration, increased basal intracellular calcium concentration ($[Ca^{2+}]_i$), inflammation, and activation of the Rho-A/Rho-associated kinase (ROCK) signaling pathway are all important mechanisms in the development

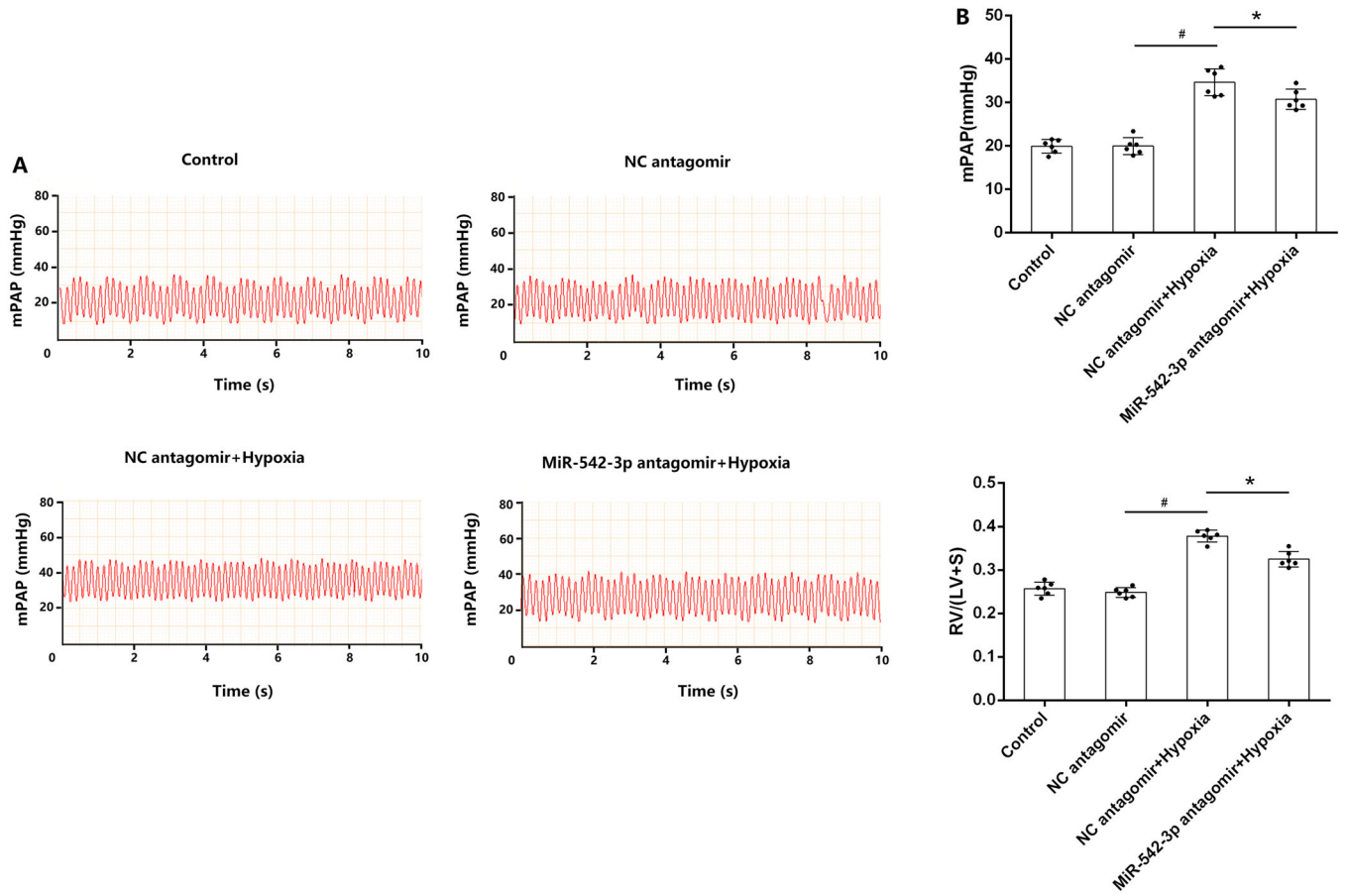

FIGURE 5 | Effects of MiR-542-3p on hemodynamics and right ventricular index in rats under hypoxic conditions. Changes of mPAP and [RV/(LV + S)] in four groups of rats (A and B). Data are expressed as means ± standard. $n = 6$; $^{\#}p < 0.05$ compared with NC antagomir. $^{*}p < 0.05$ compared with NC antagomir + hypoxia group. LV = left ventricular; mPAP = Mean pulmonary artery pressure; RV = right ventricular; S = septum; 1 mmHg = 0.133 kPa.

of HPH. PASMCs, a major component of the pulmonary vasculature, are key players in hypoxic pulmonary vascular remodeling. Mature PASMCs are non-terminally differentiated cells with significant plasticity. The plasticity of PASMCs depends on changes in environmental signals and perceived extracellular signals. Under normal physiological conditions, they have a predominantly contractile phenotype, contain abundant myofilaments, and possess a strong contractile capacity. In contrast, under pathological conditions such as hypoxia, PASMCs can undergo a phenotypic transition from a contractile phenotype to a synthetic phenotype. PASMCs in the synthetic phenotype showed a significant decrease in myofilament content and a significant increase in proliferation and migration capacity [17–19]. Therefore, it is important to explore the pathway through which hypoxia contributes to phenotypic transition in PASMCs to clarify the pathogenesis of HPH.

The phenotype of smooth muscle cells (SMCs) is regulated in vivo by a variety of signals, but the specific regulatory mechanisms remain unknown. It is widely recognized that epigenetic modifications are key processes that regulate cell differentiation and expression of specific marker genes [20]. Myocardin is currently the most potent eukaryotic transcriptional activator that binds to serum response factor (SRF) and plays a key role in the phenotypic regulation of vascular smooth muscle cells (VSMCs) [21, 22]. In Myocardin knockout mice, impaired development of VSMCs causes the mice to die on Embryonic Day 10.5, suggesting that Myocardin is one of the key molecules essential for the growth and development of VSMCs [23]. Many factors can be involved in the regulation of VSMCs phenotype by modulating Myocardin expression and interaction with SRF, but the exact mechanism is not clear.

ILK is a serine/threonine protein kinase that mediates signaling by interacting with the cytoplasmic structural domains of integrin receptor β1 and β3 subunits [24]. ILK binds to parvin and PINCH proteins to form IPP intracellular multiprotein complexes attached to adhesion spots. The IPP complex connects the extracellular matrix to the cytoskeleton and participates in bidirectional signaling between the extracellular matrix and the cell, causing the activation of multiple signaling pathways for cell proliferation, migration, and survival [25]. It has been shown that in a rat carotid balloon injury model, ILK expression was significantly reduced and accompanied by increased proliferation and migration of VSMCs [26]. ILK is one of the genes essential for maintaining the contractile phenotype of VSMCs. Our previous studies have shown that PDGF-BB can contribute to the phenotypic transition of VSMCs by inhibiting the ILK signaling pathway [27]. In addition, we also found that early hypoxia induces a decrease in ILK kinase activity, which in turn decreases the binding of Myocardin to the promoter of the SM α-actin gene, thereby contributing to the phenotypic

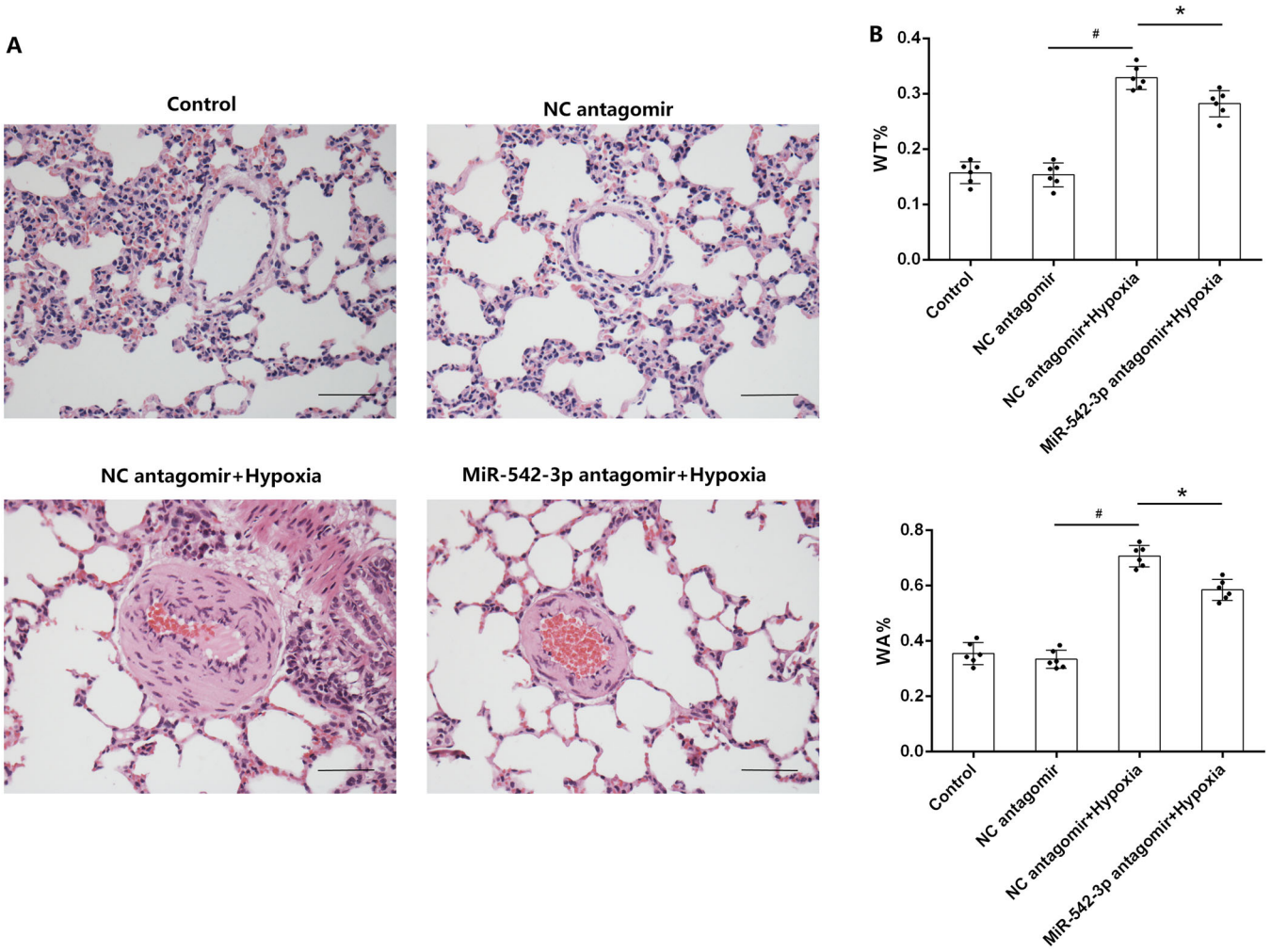

FIGURE 6 | Effects of MiR-542-3p on pulmonary vascular remodeling in rats under hypoxic conditions. Hematoxylin and eosin staining of pulmonary arteries (scale bar, 50 μm) (A). Percentage of medial wall thickness (WT%) and medial wall area (WA%) of pulmonary arteries (B). Data are expressed as means ± standard. $n = 6$; $^{\#}p < 0.05$ compared with NC antagomir. $^{*}p < 0.05$ compared with NC antagomir + hypoxia group.

transition of PASMCs at the gene level. Chronic hypoxia reduces ILK and Myocardin expression, and reduced ILK expression reduces Myocardin levels, thereby contributing to the phenotypic transition of PASMCs at the protein level [4]. However, the pathway through which hypoxia reduces ILK expression remains unknown.

microRNAs (MiRNAs) are a class of endogenous small noncoding RNAs that act as central mediators of gene expression and are involved in many important biological processes, including cell proliferation, apoptosis and metabolism [28]. It has been shown that miR-204 expression is downregulated in PH patients and pulmonary arteries of MCT-induced PH rats, and that nebulization with miR-204 mimics reverses MCT-induced PH by inhibiting the proliferation of PASMCs and promoting their apoptosis [29]. Another study showed that miR-328 expression was downregulated in HPH animal models and PH patients, and overexpression of miR-328 significantly reversed hypoxia-induced increases in right ventricular systolic pressure (RVSP) and pulmonary artery wall thickness. The underlying mechanism may be related to the regulation of insulin-like growth factor 1 receptor, L-type calcium channel-α1C expression [30]. Notably, some studies have referred to MiRNAs regulated by hypoxia as hypoxia-associated MiRNAs. Hypoxia-associated MiRNAs mediate the regulation of hypoxia-associated phenotype in VSMCs [31–33]. For example, under hypoxic conditions, miR-9, miR-214, and miR-322 expression was upregulated and miR-103 and miR-107 expression was downregulated and promoted hypoxia-induced proliferation of VSMCs [34–37]. Another study showed that miR-449a-5p was downregulated in HPH animal models and PASMCs, and that it could be involved in the development of HPH by regulating the phenotype and metabolic pathways of PASMCs through targeting the myc gene, causing their over-proliferation [38]. These findings suggest that MiRNAs may play an important role in the pathogenesis of pulmonary vascular remodeling.

With the deeper study of MiRNA function, researchers found that it is also an important way to regulate ILK expression. We found that MiR-542-3p binds to the 3′-UTR region of ILK coding genes as predicted by TargetScans biology software. It has been shown that ILK is a target gene of MiR-542-3p, and overexpression of MiR-542-3p can promote apoptosis of osteosarcoma cells by downregulating the expression of ILK, and

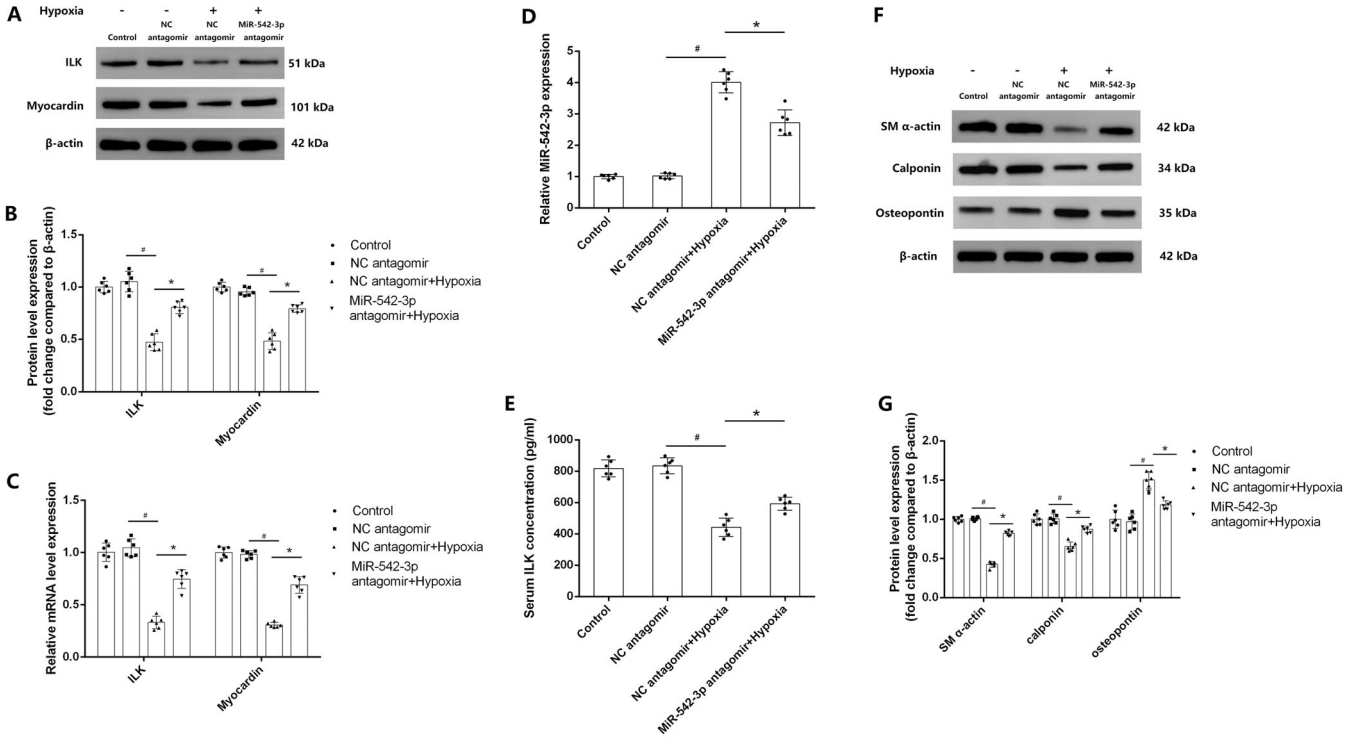

FIGURE 7 | Effects of MiR-542-3p on ILK, Myocardin expression, serum ILK concentration, and phenotype transition under hypoxic conditions in pulmonary arteries. Representative Western blots (A). Quantification of ILK and Myocardin by densitometry (B). Changes in mRNA expression of ILK and Myocardin (C). Relative expression of MiR-542-3p using Real-time quantitative PCR (D). Changes in serum ILK concentration using ELISA (E). Representative Western blots (F and G). Data are expressed as means ± standard deviation. $n = 6$; $^{\#}p < 0.05$ compared with NC antagomir. $^{*}p < 0.05$ compared with NC antagomir + hypoxia group.

inhibit their cell proliferation, migration, and invasion [39]. Moreover, MiR-542-3p levels were significantly elevated in COPD patients, and their elevation was more pronounced in critically ill COPD patients [8]. This suggests that hypoxia may regulate MiR-542-3p levels.

In this study, we found that hypoxia upregulated MiR-542-3p expression, and MiR-542-3p mimics downregulated ILK expression in PASMCs. We also found that ILK was a direct target of MiR-542-3p in PASMCs. This suggests that MiR-542-3p may be an important upstream factor regulating the phenotypic transition of PASMCs. To further validate the effects of MiR-542-3p on phenotypic transition, proliferation, and migration of PASMCs under hypoxic conditions, we transfected PASMCs using MiR-542-3p inhibitor for subsequent experiments. We found that MiR-542-3p reversed hypoxia-induced reduction of ILK and Myocardin expression in PASMCs and phenotypic transition, proliferation, and migration of PASMCs. We performed additional animal experiments to further validate the role of MiR-542-3p in pulmonary vascular remodeling. We found that MiR-542-3p reversed hypoxia-induced pulmonary vascular remodeling and also reversed hypoxia-induced reduction in ILK and Myocardin expression in rat pulmonary arteries. This suggests that MiR-542-3p may regulate hypoxia-induced pulmonary vascular remodeling by decreasing ILK and Myocardin expression.

In conclusion, we found that hypoxia induced an increase in MiR-542-3p expression, which caused an increase in binding to ILK gene and negatively regulated ILK expression. This in turn caused a decrease in Myocardin expression leading to phenotypic transition, proliferation, and increased migration of PASMCs, causing hypoxic pulmonary vascular remodeling and ultimately leading to HPH.

Author Contributions

Linqing Li and Weining Zhou contributed equally to this manuscript. Linqing Li and Weining Zhou conducted the experiments and wrote the manuscript. Jiantong Hou designed the study. Qingrong Ji, Xianzhao Zhang, Ni Yang, Kaiyou Song, Shunpeng Hu, Cunfei Liu, Zhihong Ou, Fengwei Zhang, and Yuda Wei analyzed the data and edited the manuscript.

Acknowledgments

The authors have nothing to report.

Ethics Statement

All animal experiments complied with the ARRIVE guidelines and were performed in accordance with the National Institutes of Health Guide for the Care and Use of Laboratory Animals. This study was approved by the Ethics Review Board for Animal Studies at the Institute of Linyi People's Hospital, Linyi, China.

Conflicts of Interest

The authors declare no conflicts of interest.

Data Availability Statement

The data sets used and/or analyzed during the present study are available from the corresponding author upon reasonable request.

References

1. D. B. Badesch, G. E. Raskob, C. G. Elliott, et al., "Pulmonary Arterial Hypertension: Baseline Characteristics From the REVEAL Registry," *Chest* 137, no. 2 (2010): 376–387.

2. M. M. Zucker, L. Wujak, A. Gungl, et al., "LRP1 Promotes Synthetic Phenotype of Pulmonary Artery Smooth Muscle Cells in Pulmonary Hypertension," *Biochimica et Biophysica Acta (BBA)—Molecular Basis of Disease* 1865, no. 6 (2019): 1604–1616.

3. P. C. Mcdonald, A. B. Fielding, and S. Dedhar, "Integrin-Linked Kinase—Essential Roles in Physiology and Cancer Biology," *Journal of Cell Science* 121, no. Pt 19 (2008): 3121–3132.

4. J. Hou, B. Liu, B. Zhu, et al., "Role of Integrin-Linked Kinase in the Hypoxia-Induced Phenotypic Transition of Pulmonary Artery Smooth Muscle Cells Implications for Hypoxic Pulmonary Hypertension," *Experimental Cell Research* 382 (2019): 111476.

5. D. P. Bartel, "microRNAs: Genomics, Biogenesis, Mechanism, and Function," *Cell* 116, no. 2 (2004): 281–297.

6. J. Bienertova-Vasku, J. Novak, and A. Vasku, "MicroRNAs in Pulmonary Arterial Hypertension: Pathogenesis, Diagnosis and Treatment," *Journal of the American Society of Hypertension* 9, no. 3 (2015): 221–234.

7. J. Lee and H. Kang, "Hypoxia Promotes Vascular Smooth Muscle Cell Proliferation Through MicroRNA-Mediated Suppression of Cyclin-Dependent Kinase Inhibitors," *Cells* 8, no. 8 (2019): 802.

8. R. Farre-Garros, J. Y. Lee, S. A. Natanek, et al., "Quadriceps miR-542-3p and -5p are Elevated in COPD and Reduce Function by Inhibiting Ribosomal and Protein Synthesis," *Journal of Applied Physiology* 126, no. 6 (2019): 1514–1524.

9. W. Seeger, Y. Adir, J. A. Barberà, et al., "Pulmonary Hypertension in Chronic Lung Diseases," *Journal of the American College of Cardiology* 62, no. S25 (2013): D109–D116.

10. E. Melicoff, D. Hayes, Jr., and C. Benden, "Lung Transplantation as an Intervention for Pediatric Pulmonary Hypertension," *Pediatric Pulmonology* 56, no. 3 (2021): 587–592.

11. S. M. Arcasoy and R. M. Kotloff, "Lung Transplantation," *New England Journal of Medicine* 340, no. 14 (1999): 1081–1091.

12. G. Simonneau, I. M. Robbins, M. Beghetti, et al., "Updated Clinical Classification of Pulmonary Hypertension," *Journal of the American College of Cardiology* 54, no. S1 (2009): S43–S54.

13. B. Zhang, W. Niu, H. Y. Dong, M. L. Liu, Y. Luo, and Z. C. Li, "Hypoxia Induces Endothelialmesenchymal Transition in Pulmonary Vascular Remodeling," *International Journal of Molecular Medicine* 42, no. 1 (2018): 270–278.

14. N. C. Lopez, G. Ebensperger, E. A. Herrera, et al., "Role of the RhoA/ROCK Pathway in High-Altitude Associated Neonatal Pulmonary Hypertension in Lambs," *American Journal of Physiology-Regulatory, Integrative and Comparative Physiology* 310, no. 11 (2016): R1053–R1063.

15. S. C. Pugliese, J. M. Poth, M. A. Fini, A. Olschewski, K. C. El Kasmi, and K. R. Stenmark, "The Role of Inflammation in Hypoxic Pulmonary Hypertension: From Cellular Mechanisms to Clinical Phenotypes," *American Journal of Physiology—Lung Cellular and Molecular Physiology* 308, no. 3 (2015): L229–L252.

16. K. Suresh, L. Servinsky, H. Jiang, et al., "Reactive Oxygen Species Induced Ca^{2+} Influx via TRPV4 and Microvascular Endothelial Dysfunction in the SU5416/Hypoxia Model of Pulmonary Arterial Hypertension," *American Journal of Physiology—Lung Cellular and Molecular Physiology* 314, no. 5 (2018): L893–L907.

17. Y. Jiang, Y. Zhou, G. Peng, et al., "Topotecan Prevents Hypoxia-Induced Pulmonary Arterial Hypertension and Inhibits Hypoxia-Inducible Factor-1α and TRPC Channels," *International Journal of Biochemistry & Cell Biology* 104 (2018): 161–170.

18. W. Zhang, T. Zhu, W. Wu, et al., "LOX-1 Mediated Phenotypic Switching of Pulmonary Arterial Smooth Muscle Cells Contributes to Hypoxic Pulmonary Hypertension," *European Journal of Pharmacology* 818 (2018): 84–95.

19. X. Peng, H. X. Li, H. J. Shao, et al., "Involvement of Calcium-Sensing Receptors in Hypoxia-Induced Vascular Remodeling and Pulmonary Hypertension by Promoting Phenotypic Modulation of Small Pulmonary Arteries," *Molecular and Cellular Biochemistry* 396, no. 1–2 (2014): 87–98.

20. O. G. Mcdonald and G. K. Owens, "Programming Smooth Muscle Plasticity With Chromatin Dynamics," *Circulation Research* 100, no. 10 (2007): 1428–1441.

21. C. P. Mack and J. S. Hinson, "Regulation of Smooth Muscle Differentiation by the Myocardin Family of Serum Response Factor Co-Factors," *Journal of Thrombosis and Haemostasis* 3, no. 9 (2005): 1976–1984.

22. D. Z. Wang, P. S. Chang, Z. Wang, et al., "Activation of Cardiac Gene Expression by Myocardin, a Transcriptional Cofactor for Serum Response Factor," *Cell* 105, no. 7 (2001): 851–862.

23. S. Li, D. Z. Wang, Z. Wang, J. A. Richardson, and E. N. Olson, "The Serum Response Factor Coactivator Myocardin Is Required for Vascular Smooth Muscle Development," *Proceedings of the National Academy of Sciences* 100, no. 16 (2003): 9366–9370.

24. J. M. Pasquet, M. Noury, and A. Nurden, "Evidence That the Platelet Integrin αIIbβ3 Is Regulated by the Integrin-Linked Kinase, ILK, in a PI3-Kinase Dependent Pathway," *Thrombosis and Haemostasis* 88, no. 1 (2002): 115–122.

25. F. G. Giancotti and E. Ruoslahti, "Integrin Signaling," *Science* 285, no. 5430 (1999): 1028–1033.

26. B. Ho, G. Hou, J. G. Pickering, G. Hannigan, B. L. Langille, and M. P. Bendeck, "Integrin-Linked Kinase in the Vascular Smooth Muscle Cell Response to Injury," *American Journal of Pathology* 173, no. 1 (2008): 278–288.

27. G. Yan, Q. Wang, S. Hu, et al., "Digoxin Inhibits PDGF-BB-Induced VSMC Proliferation and Migration Through an Increase in ILK Signaling and Attenuates Neointima Formation Following Carotid Injury," *International Journal of Molecular Medicine* 36, no. 4 (2015): 1001–1011.

28. A. Mohr and J. Mott, "Overview of MicroRNA Biology," *Seminars in Liver Disease* 35, no. 1 (2015): 003–011.

29. A. Courboulin, R. Paulin, N. J. Giguère, et al., "Role for miR-204 in Human Pulmonary Arterial Hypertension," *Journal of Experimental Medicine* 208, no. 3 (2011): 535–548.

30. L. Guo, Z. Qiu, L. Wei, et al., "The MicroRNA-328 Regulates Hypoxic Pulmonary Hypertension by Targeting at Insulin Growth Factor 1 Receptor and L-Type Calcium Channel-α1C," *Hypertension* 59, no. 5 (2012): 1006–1013.

31. J. Loscalzo, "The Cellular Response to Hypoxia: Tuning the System With MicroRNAs," *Journal of Clinical Investigation* 120, no. 11 (2010): 3815–3817.

32. H. Kang and A. Hata, "MicroRNA Regulation of Smooth Muscle Gene Expression and Phenotype," *Current Opinion in Hematology* 19, no. 3 (2012): 224–231.

33. J. Lee, J. Heo, and H. Kang, "miR-92b-3p-TSC1 Axis Is Critical for mTOR Signaling-Mediated Vascular Smooth Muscle Cell Proliferation Induced by Hypoxia," *Cell Death & Differentiation* 26, no. 9 (2019): 1782–1795.

34. F. Shan, J. Li, and Q. Y. Huang, "HIF-1 Alpha-Induced Up-Regulation of miR-9 Contributes to Phenotypic Modulation in

Pulmonary Artery Smooth Muscle Cells During Hypoxia," *Journal of Cellular Physiology* 229, no. 10 (2014): 1511–1520.

35. H. Liu, T. Yin, W. Yan, et al., "Dysregulation of MicroRNA-214 and PTEN Contributes to the Pathogenesis of Hypoxic Pulmonary Hypertension," *International Journal of Chronic Obstructive Pulmonary Disease* 12 (2017): 1781–1791.

36. Y. Zeng, H. Liu, K. Kang, et al., "Hypoxia Inducible Factor-1 Mediates Expression of miR-322: Potential Role in Proliferation and Migration of Pulmonary Arterial Smooth Muscle Cells," *Scientific Reports* 5 (2015): 12098.

37. B. Deng, J. Du, R. Hu, et al., "MicroRNA-103/107 Is Involved in Hypoxia-Induced Proliferation of Pulmonary Arterial Smooth Muscle Cells by Targeting HIF-1β," *Life Sciences* 147 (2016): 117–124.

38. C. Zhang, C. Ma, L. Zhang, et al., "MiR-449a-5p Mediates Mitochondrial Dysfunction and Phenotypic Transition by Targeting Myc in Pulmonary Arterial Smooth Muscle Cells," *Journal of Molecular Medicine* 97, no. 3 (2019): 409–422.

39. W. Cai, Y. Xu, W. Zuo, and Z. Su, "MicroR-542-3p Can Mediate ILK and Further Inhibit Cell Proliferation, Migration and Invasion in Osteosarcoma Cells," *Aging* 11, no. 1 (2019): 18–32.

Supporting Information

Additional supporting information can be found online in the Supporting Information section.